Partial oxidation of methane on Pt/Ce–ZrO$_2$ catalysts

L.V. Mattos [a,1], E.R. de Oliveira [b], P.D. Resende [a,1], F.B. Noronha [a,1], F.B. Passos [b,*]

[a] *Instituto Nacional de Tecnologia (INT), Av. Venezuela 82, 20081-310 Rio de Janeiro, Brazil*
[b] *Departamento de Engenharia Química e Programa de Pós-Graduação em Química Orgânica,*
Universidade Federal Fluminense, Rua Passos da Pátria, 156, 24210-240 Niterói, Brazil

Abstract

The mechanism of partial oxidation of methane was studied on Pt/Al$_2$O$_3$, Pt/ZrO$_2$ and Pt/Ce–ZrO$_2$ catalysts. The reducibility and oxygen transfer capacity were evaluated by temperature programmed reduction (TPR) and oxygen storage capacity (OSC). The effect of the support on the cleaning mechanism of the catalyst surface was investigated by the sequence of CH$_4$/O$_2$ pulses. Moreover, temperature programmed surface reaction (TPSR) measurements were performed to evaluate the reaction mechanism. Pt/Ce–ZrO$_2$ catalysts proved to be more active, stable and selective than Pt/Al$_2$O$_3$ and Pt/ZrO$_2$ catalysts. The results were explained by the higher reducibility and oxygen storage/release capacity of Pt/Ce–ZrO$_2$ catalysts, which allowed a continuous removal of carbonaceous deposits from the active sites, favoring the stability and activity of the catalysts, as revealed by the CH$_4$/O$_2$ pulses. TPSR experiments showed that the partial oxidation of methane proceeded through a two-step mechanism.
© 2002 Elsevier Science B.V. All rights reserved.

Keywords: Partial oxidation of methane; Pt/Ce–ZrO$_2$ catalysts; Oxygen storage capacity

1. Introduction

The large known reserves of natural gas and the need to reduce the dependence on petroleum as feedstock have led to intense research on natural gas conversion into transportation fuel such as gasoline and diesel. The classical gas to liquids technology (GTL) includes the conversion of natural gas to synthesis gas followed by Fischer–Tropsch synthesis [1]. The economical feasibility of this route is highly dependent on the costs of synthesis gas manufacture. Steam-reforming is the leading technology for synthesis gas production, but it requires a large amount of heat addition, and the ratio of hydrogen to carbon monoxide that results is too high for fuel synthesis [2]. Methane partial oxidation is an alternative route that may reduce the costs of synthesis gas production. It is energy efficient, produces the H$_2$/CO ratio necessary to GTL process and if associated to a competitive way for separating oxygen from air (such as selective membranes), it will probably be the choice for producing synthesis gas [3–9].

A two-step mechanism has been proposed for the partial oxidation of methane [10–12]. According to this mechanism, in the first step, combustion of methane takes place, producing CO$_2$ and H$_2$O. In the second one, synthesis gas is produced via carbon dioxide and steam-reforming reaction of unreacted methane.

Ce–ZrO$_2$ supported Pt catalysts have been investigated previously in the CO$_2$-reforming of methane [13–15]. The Pt catalysts supported on ceria-doped zirconia exhibited higher activity and stability than

* Corresponding author. Fax: +55-21-2717-4446.
E-mail addresses: fabiobel@int.gov.br (F.B. Noronha),
fbpassos@engenharia.uff.br (F.B. Passos).
[1] Fax: +55-21-2206-1051.

Pt/Al_2O_3 catalysts [13]. The enhancement of the activity and the stability on the CO_2-reforming reaction has been attributed to the high amount of oxygen vacancies near the metal particles. The reducibility and oxygen transfer capacity of $Ce–ZrO_2$ have shown to be fundamental in keeping the active phase surface free of carbonaceous deposits [15].

Then, the aim of this work is to study the mechanism of the partial oxidation of methane on the $Pt/Ce–ZrO_2$ catalysts, evaluating the effect of support reducibility and oxygen transfer capacity on the progress of partial oxidation, comparing with CO_2-reforming of methane on the same catalysts. Temperature programmed reduction (TPR) and oxygen storage capacity (OSC) measurements were performed to characterize the reducibility and the oxygen transfer capacity of the samples. A series of CH_4/O_2 pulses were used to study the effect of the support on the cleaning mechanism of the catalyst surface. Furthermore, temperature programmed surface reaction (TPSR) experiments provided insights on the reaction mechanism.

2. Experimental

2.1. Catalyst preparation

Al_2O_3 and ZrO_2 supports were prepared by calcination of a γ-alumina (Engelhard Corporation Catalyst) and zirconium hydroxide (MEL Chemicals) at 1073 K for 1 h in a muffle. The $Ce_{0.75}Zr_{0.25}O_2$ support was obtained by a co-precipitation method [16]. An aqueous solution of cerium(IV) ammonium nitrate and zirconium nitrate (Aldrich) was prepared with 75 and 25% (mol%) of CeO_2 and ZrO_2, respectively. Then, the ceria and zirconium hydroxides were co-precipitated by the addition of an excess of ammonium hydroxide. Finally, the precipitate was washed with distilled water and calcined at 1073 K for 1 h in a muffle. Then, the catalysts were prepared by incipient wetness impregnation of the supports with an aqueous solution of H_2PtCl_6 (Aldrich) and were dried at 393 K. The samples Pt/ZrO_2 and $Pt/Ce_{0.75}Zr_{0.25}O_2$ were calcined under air (50 cm^3/min) at 673 K for 2 h. The sample Pt/Al_2O_3 was calcined under air (50 cm^3/min) at 673 K (Pt/Al_2O_3 (673)) or 973 K (Pt/Al_2O_3 (973)) for 2 h. All samples contained 1.5 wt.% of platinum.

2.2. X-ray diffraction (XRD)

XRD measurements were made using a RIGAKU diffractometer with a Cu Kα radiation. After calcination at 1073 K of ZrO_2 and $Ce_{0.75}Zr_{0.25}O_2$ supports, the XRD data were collected at 0.04° per step with integration times of 1 s per step.

2.3. Temperature programmed reduction (TPR)

TPR measurements were carried out in a microreactor coupled to a quadrupole mass spectrometer (Balzers, Omnistar). The samples (300 mg) were dehydrated at 423 K for 30 min in a He flow prior to reduction. After cooling to room temperature, a mixture of 5% H_2 in Ar flowed through the sample at 30 cm^3/min, raising the temperature at a heating rate of 10 K/min up to 1273 K.

2.4. OSC

OSC measurements were carried out in a microreactor coupled to a quadrupole mass spectrometer (Balzers, Omnistar). The samples were reduced under H_2 at 773 K for 1 h and heated to 1073 K in flowing He. Then, the samples were cooled to 723 K and a 5% O_2/He mixture was passed through the catalyst until the oxygen uptake was finished. The reactor was purged with He and the dead volume was obtained by switching the gas to the 5% O_2/He mixture. Finally, N_2 pulses were injected in order to calculate the amount of oxygen consumed on the catalysts taking into account a previous calibration of the mass spectrometer.

2.5. CO chemisorption

The dispersion was calculated from CO chemisorption by using pulses of a mixture containing 5% CO/Ar at room temperature. This experiment was performed on the same apparatus described to the TPR measurements and the samples were submitted to the same pretreatment used in OSC experiments.

2.6. TPSR

TPSR experiments were performed in the same apparatus used for TPR. After reduction at 773 K under H_2 for 1 h, the sample (300 mg) was purged in

He at 1073 K for 30 min, and cooled to room temperature. Then the sample was submitted to a flow of $CH_4/O_2/He$ (2:1:27) at 30 cm^3/min while the temperature was raised up to 1073 K at a heating rate of 20 K/min.

2.7. Reaction conditions

Reaction was performed in a quartz reactor at atmospheric pressure. Prior to reaction, the catalyst was reduced under H_2 at 773 K for 1 h and then heated to 1073 K under N_2. The reaction was carried out: (i) at 673 K and WHSV = 520 h^{-1} over $Pt/Ce_{0.75}Zr_{0.25}O_2$ catalyst and (ii) at 1073 K and WHSV = 520 h^{-1} over all catalysts. At both temperatures, a reactant mixture with CH_4/O_2 ratio of 2:1 was used with a flow rate of 100 cm^3/min. The exit gases were analyzed using a gas chromatograph (Agilent 6890) equipped with a thermal conductivity detector and a CP-carboplot column (Chrompack).

2.8. CH_4 and O_2 pulse experiments

Pulses experiments using CH_4 or O_2 were performed in a micro-reactor coupled to a quadrupole mass spectrometer (Balzers, Omnistar) using 50 mg of catalyst. The samples were reduced under H_2 at 773 K for 1 h. After reduction, the samples were heated to 1073 K in flowing He and then were exposed to sequences of $CH_4/O_2/CH_4$ pulses (500 μl pulses). Finally, the N_2 pulses were injected in order to calculate the CH_4, CO and H_2 moles using a conversion factor that was determined from a previous calibration of the mass spectrometer.

3. Results and discussion

3.1. Catalyst characterization

The XRD data obtained for ZrO_2 and $Ce_{0.75}Zr_{0.25}O_2$ supports are presented in Fig. 1. After calcination at 1073 K, essentially the presence of monoclinic phase (JCPDS 13-307) was observed for ZrO_2 support. Noronha et al. [13] observed the same result in a Pt/ZrO_2 catalyst calcined at 1073 K. The addition of 75% of CeO_2 led to the appearance of peaks at
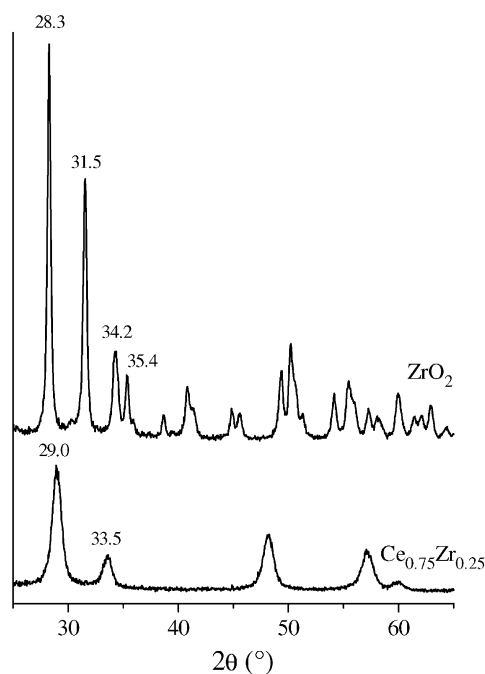

Fig. 1. XRD patterns of ZrO_2 and $Ce_{0.75}Zr_{0.25}O_2$ supports.

$2\theta = 29.0°$ and $33.5°$, which indicates that zirconia was incorporated into CeO_2 lattice and formed a solid solution with a cubic symmetry. Noronha et al. [13] also obtained a cubic Ce–Zr solid solution for $Pt/Ce_{0.75}Zr_{0.25}O_2$ catalyst calcined at 1073 K. Hori et al. [16] studied the effect of ZrO_2 addition to CeO_2 on the phase composition of Pt/Ce–ZrO_2 catalysts, using XRD experiments. Their discussion was based on the peaks at $2\theta = 28.6°$ and $33.1°$ for cubic CeO_2 and 30.2, 34.5 and 35.3° for tetragonal ZrO_2. They observed that the addition of 25% of ZrO_2 did not result in a separate zirconia phase, but the ceria peaks shifted from $2\theta = 28.6°$ to 29.0° and from $2\theta = 33.1°$ to 33.5°. According to these authors, this shift is indicative of change in lattice parameter, and it is evident that CeO_2 and ZrO_2 formed a solid solution.

The dispersion of the catalysts calculated from CO chemisorption experiments is listed in Table 1. Pt/Al_2O_3 (973) and $Pt/Ce_{0.75}Zr_{0.25}O_2$ catalysts exhibited approximately the same dispersion (around 10%) whereas the Pt/Al_2O_3 (673) and Pt/ZrO_2 catalysts showed higher dispersions.

Table 1
Dispersion calculated from the CO chemisorption at 298 K, H_2 uptakes during TPR experiments and O_2 uptakes measured at 723 K

Catalyst	Dispersion (%)	H_2 uptake (μmol/$g_{catalyst}$)	O_2 uptake (μmol/$g_{catalyst}$)
Pt/Al$_2$O$_3$ (673)	48	153.1	0.0
Pt/Al$_2$O$_3$ (973)	10	–	0.0
Pt/ZrO$_2$	26	166.7 (30.7)[a]	8.5
Pt/Ce$_{0.75}$Zr$_{0.25}$O$_2$	9	1467.9 (1103.5)[a]	625.6

[a] H_2 uptake of the corresponding support (without Pt).

3.2. Catalyst reducibility

The reducibility of the catalysts was measured by TPR and OSC experiments.

The TPR profiles of the ZrO$_2$ and Ce$_{0.75}$Zr$_{0.25}$O$_2$ supports are shown in Fig. 2. For the ZrO$_2$ support, a slight reduction around 931 K was observed. The Ce$_{0.75}$Zr$_{0.25}$O$_2$ support presented a strong H_2 consumption at 854 K and a slight consumption at 1150 K. Furthermore, the H_2 uptake (Table 1) was higher for Ce$_{0.75}$Zr$_{0.25}$O$_2$ support.

Fig. 2 also shows the TPR profiles of the Pt/ZrO$_2$ and Pt/Ce$_{0.75}$Zr$_{0.25}$O$_2$ catalysts. The Pt/ZrO$_2$ catalyst showed H_2 uptakes at 477 K related to PtO$_2$ reduction, according to stoichiometric calculation, and to ZrO$_2$ reduction at 659 K. This is attributed to the PtO$_2$ reduction and the promoted support reduction through spillover of hydrogen species [17]. Pt/Ce$_{0.75}$Zr$_{0.25}$O$_2$ catalyst exhibited a dominant low temperature reduction feature and it was no more observed the H_2 consumption at high temperature due to the reduction of support. This peak is ascribed to reduction of PtO$_2$ and Ce$_{0.75}$Zr$_{0.25}$O$_2$ support. Moreover, the H_2 consumption was higher for Pt/Ce$_{0.75}$Zr$_{0.25}$O$_2$ catalyst (Table 1). Comparing these results with that obtained for Ce$_{0.75}$Zr$_{0.25}$O$_2$ support, we may conclude the addition of Pt promotes the reduction of support [17].

Table 1 presents the oxygen uptakes measured for the catalysts. The O_2 consumption obtained for Pt/Ce$_{0.75}$Zr$_{0.25}$O$_2$ catalyst is similar to those reported in the literature [18–20]. The amount of Ce^{3+} estimated from O_2 uptake was around 53%. This result is consistent with H_2 uptakes during TPR that indicated 47% of Ce^{3+}, after reduction. The OSC of the

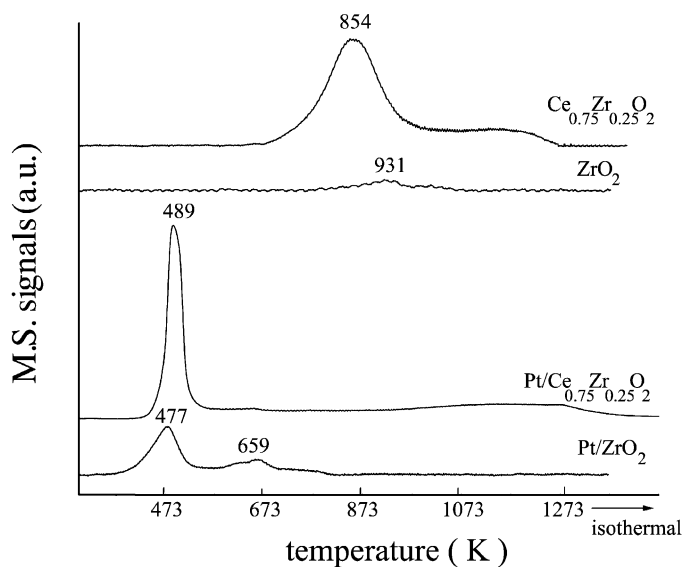Fig. 2. TPR profile of supports (ZrO$_2$ and Ce$_{0.75}$Zr$_{0.25}$O$_2$) and catalysts (Pt/ZrO$_2$ and Pt/Ce$_{0.75}$Zr$_{0.25}$O$_2$).

$Pt/Ce_{0.75}Zr_{0.25}O_2$ catalyst is considerably higher than the one of the Pt/ZrO_2 and Pt/Al_2O_3 (973) catalysts (Table 1). Several studies reported that cerium oxide have a very high oxygen exchange capacity [17,21]. This capacity is associated to the ability of cerium to act as an oxygen buffer by storing/releasing O_2 due to the Ce^{4+}/Ce^{3+} redox couple [21]. The incorporation of ZrO_2 into CeO_2 lattice promoted the CeO_2 redox properties. The presence of ZrO_2 strongly increased the oxygen vacancies of the support due to the high oxygen mobility of the solid solution formed, which was identified by our XRD data.

3.3. Partial oxidation of methane

3.3.1. Particle size effect

The catalytic activity of the Pt/Al_2O_3 catalysts calcined at different temperatures on the partial oxidation of methane at 1073 K is presented in Figs. 3 and 4. The evolution of CH_4 conversion and H_2 selectivity as a function of time on stream (TOS) is shown in Fig. 3, while the CO and CO_2 selectivities are reported in Fig. 4.
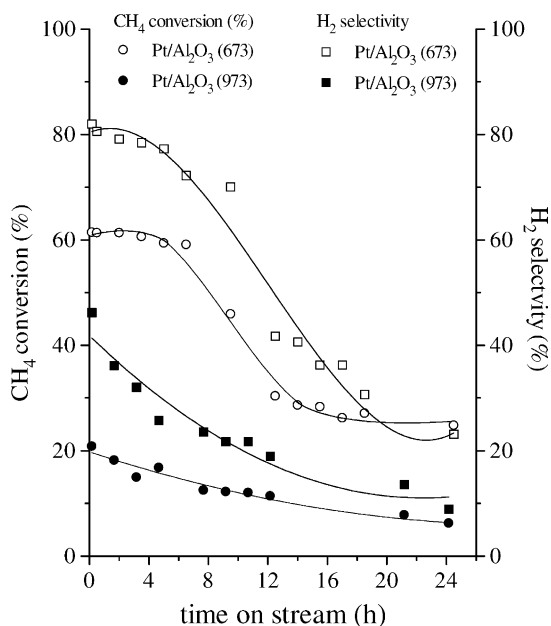

Fig. 3. CH_4 conversion and H_2 selectivity over Pt/Al_2O_3 catalyst calcined at 673 (open symbols) and 973 K (closed symbols); $T_{reaction} = 1073$ K and WHSV = 520 h^{-1}.
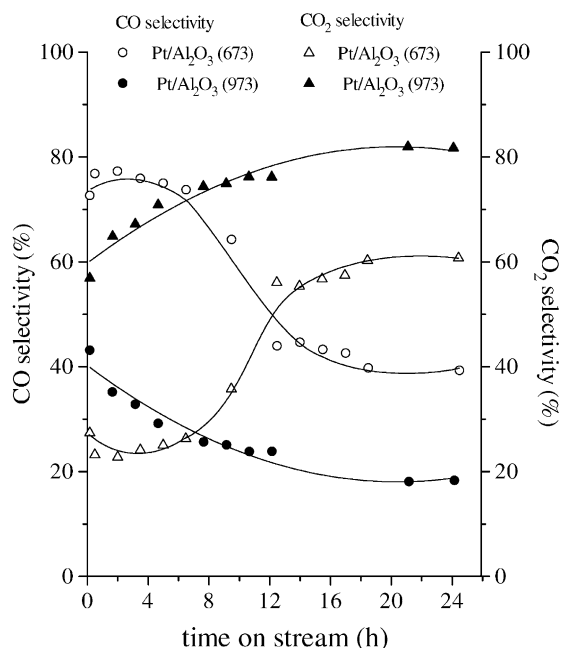

Fig. 4. CO and CO_2 selectivities over Pt/Al_2O_3 (673) (open symbols) and Pt/Al_2O_3 (973) (closed symbols) catalysts; $T_{reaction} = 1073$ K and WHSV = 520 h^{-1}.

These results show that initial conversion was higher for Pt/Al_2O_3 (673) catalyst, indicating that the CH_4 conversion increases as the dispersion of the catalyst increases. Moreover, the selectivity to H_2 and CO was higher over Pt/Al_2O_3 (673) catalyst. Ruckenstein and Wang [22] also observed a positive effect of dispersion on partial oxidation of methane for Rh supported catalysts.

Both Al_2O_3 supported catalysts were not stable and the deactivation was stronger for Pt/Al_2O_3 (673). However, Pt/Al_2O_3 (673) exhibited a higher final activity than Pt/Al_2O_3 (973) catalyst. The H_2 and CO selectivities decreased during the run for both catalysts (Fig. 4). The decrease of CO selectivity was accompanied by the increase of CO_2 selectivity. These results can be attributed to coke deposition on the catalyst surface, which was more significant on catalysts that have higher activity.

3.3.2. Reaction mechanism and role of the support

It has been proposed that the partial oxidation of methane proceeds through a two-step mechanism [9–12]. In the first stage, combustion of methane oc-
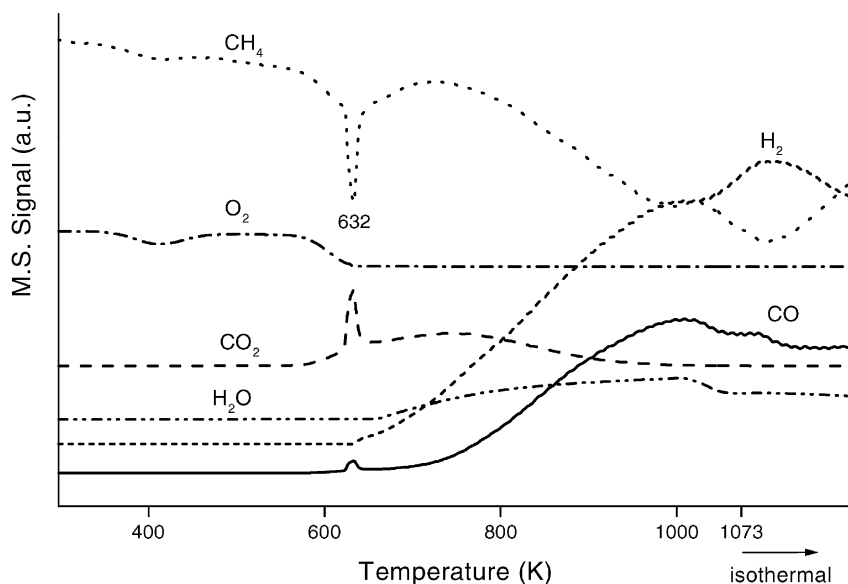
Fig. 5. TPSR profiles for $Pt/Ce_{0.75}Zr_{0.25}O_2$ catalyst.

curs producing CO_2 and H_2O. In the second step, synthesis gas is produced via carbon dioxide and steam-reforming reaction of the unreacted methane. TPSR experiments and partial oxidation of methane at low and high temperature were carried out in order to confirm this mechanism.

3.3.2.1. TPSR experiments. Fig. 5 shows the TPSR profile obtained for $Pt/Ce_{0.75}Zr_{0.25}O_2$ catalyst. The other samples showed similar profiles. The TPSR profile is consistent to the partial oxidation of methane proceeding through this two-step mechanism, as we first observe the combustion of methane followed by CO_2 and H_2O methane-reforming.

3.3.2.2. Partial oxidation of methane at low temperature. The partial oxidation was carried at 673 K on $Pt/Ce_{0.75}Zr_{0.25}O_2$ catalyst to confirm the results obtained in TPSR experiments. Fig. 6 shows CH_4 conversion and H_2 selectivity on $Pt/Ce_{0.75}Zr_{0.25}O_2$ catalyst, while Fig. 7 presents CO and CO_2 selectivities on this catalyst. The results showed that the main products were CO_2 and H_2O (Figs. 6 and 7) in agreement with TPSR experiments, which indicates that combustion of methane is the first step of the partial oxidation of methane. However, Figs. 6 and 7 also reveal the

formation of CO and H_2 even at this temperature. At 673 K, the equilibrium composition calculated for the partial oxidation reaction using a O_2/CH_4 ratio of 0.5 does not predict the CO production [23,24].

The CO_2-reforming of methane is strongly influenced by the reverse water gas-shift (RWGS) reaction (Eq. (1)) [25]. This is reflected on the H_2/CO ratio
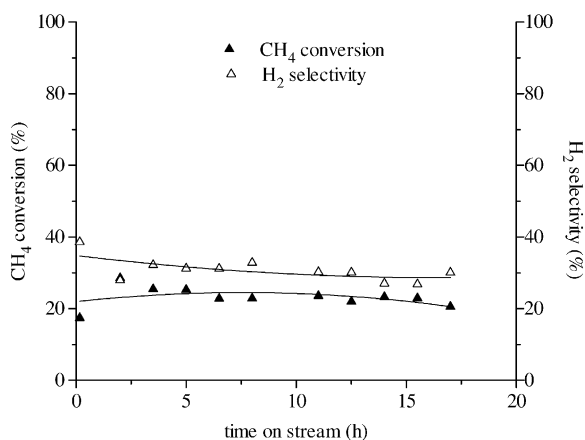

Fig. 6. CH_4 conversion (closed symbols) and H_2 selectivity (open symbols) over $Pt/Ce_{0.75}Zr_{0.25}O_2$ catalyst; $T_{reaction} = 673$ K and WHSV $= 520\,h^{-1}$.
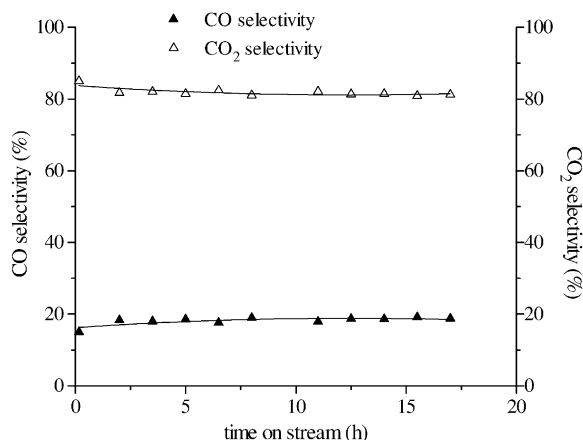
Fig. 7. CO (closed symbols) and CO_2 (open symbols) selectivities over $Pt/Ce_{0.75}Zr_{0.25}O_2$ catalyst; $T_{reaction} = 673\,K$ and $WHSV = 520\,h^{-1}$.

lower than 1.0.

$$H_2 + CO_2 \rightarrow CO + H_2O \qquad (1)$$

The thermodynamic calculations of the RWGS equilibrium for the $CH_4/CO_2 = 1/1$ at 1 atm show that CO can be formed at 673 K through this reaction. Therefore, the CO production could be attributed to the RWGS reaction, in parallel to the first step of the partial oxidation of methane. Besides, examining the TPSR profile shown in Fig. 5, we may notice the formation of CO around 650 K, which can be attributed to the RWGS reaction.

3.3.2.3. Partial oxidation of methane at high temperature.
Fig. 8 presents the methane conversion and H_2 selectivity on the partial oxidation of methane at 1073 K over Pt/ZrO_2 and $Pt/Ce_{0.75}Zr_{0.25}O_2$ catalysts. The initial CH_4 conversions were similar for both catalysts. Comparing these results with those obtained for Pt/Al_2O_3 (973) catalyst (Fig. 3), it is clear that Pt/ZrO_2 and $Pt/Ce_{0.75}Zr_{0.25}O_2$ showed higher activities. Moreover, Pt/ZrO_2 strongly deactivated, while $Pt/Ce_{0.75}Zr_{0.25}O_2$ catalyst practically has not lost the activity after 24 h TOS.

The H_2 selectivity followed the same trend as CH_4 conversion and strongly decreased with time for Pt/ZrO_2 catalyst whereas it remained unchanged for $Pt/Ce_{0.75}Zr_{0.25}O_2$ catalyst. Furthermore, a significant change in the selectivity towards CO and CO_2 was observed for the Pt/ZrO_2 catalyst during the reaction
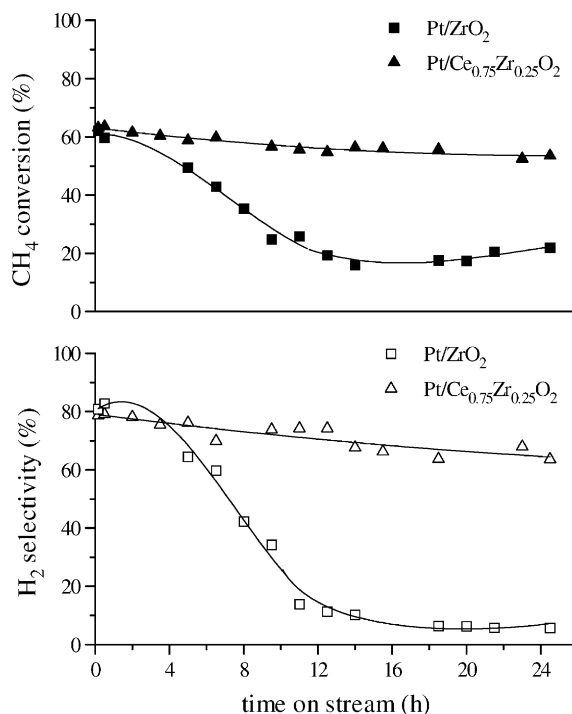

Fig. 8. CH_4 conversion (closed symbols) and H_2 selectivity (open symbols) over Pt/ZrO_2 and $Pt/Ce_{0.75}Zr_{0.25}O_2$ catalysts; $T_{reaction} = 1073\,K$ and $WHSV = 520\,h^{-1}$.

(Fig. 9). The production of CO_2 increased and the selectivity to CO decreased as the CH_4 conversion decreased. Thus the deactivation of these catalysts was followed by the increase of CO_2 selectivity. This effect is less significant for $Pt/Ce_{0.75}Zr_{0.25}O_2$ catalyst. The Pt/ZrO_2 catalyst presented the same catalytic behavior of Pt/Al_2O_3 (973) catalyst (Figs. 3 and 9).

These results could be explained taking into account the two-step mechanism of the partial oxidation of methane. Since the production of carbon and CO_2 increased on the Pt/Al_2O_3 (973) and Pt/ZrO_2 catalysts during the reaction, the second step of the mechanism was inhibited.

3.3.2.4. The role of support on the reaction mechanism.
The CO_2-reforming of methane over supported transition metals involves the methane activation and the CO_2 dissociation [26,27]. When the rate of methane decomposition and the CO_2 dissociation are unbalanced, carbon builds up over the surface. The carbon deposition under CO_2-reforming of CH_4
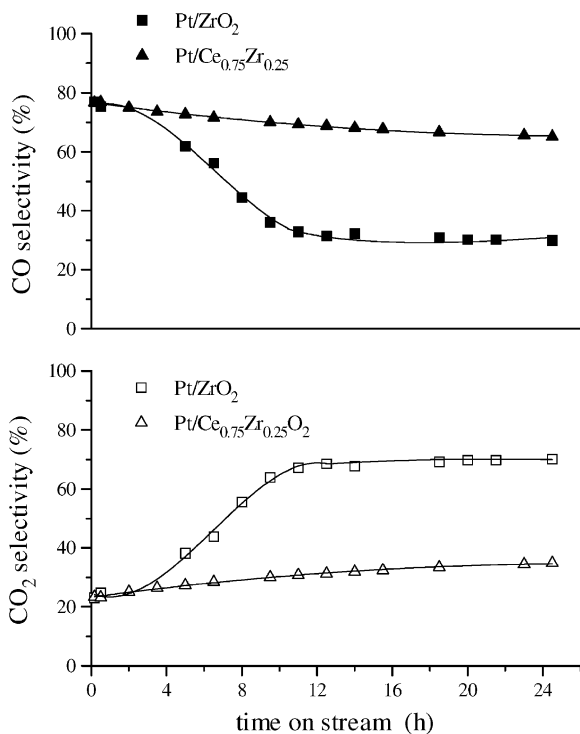
Fig. 9. CO (closed symbols) and CO_2 (open symbols) selectivities over Pt/ZrO_2 and $Pt/Ce_{0.75}Zr_{0.25}O_2$ catalysts; $T_{reaction} = 1073$ K and WHSV $= 520 \, h^{-1}$.

is strongly related to the activity of the metals for CO_2 dissociation [28,29]. Ru and Rh are very active for CO_2 dissociation and consequently no carbon deposition is observed. On the other hand, Pt is less effective in activating CO_2 and severe carbon formation takes place. Therefore, the support plays an important role on the CO_2-reforming of methane over supported Pt catalysts.

Pt/ZrO_2 catalysts exhibit a very high stability on the dry-reforming reaction whereas a strong deactivation is observed on Pt/Al_2O_3 and Pt/SiO_2 catalysts [28–31]. The stable behavior of the Pt/ZrO_2 catalyst has been associated with the low carbon formation.

Several studies have been reported concerning the CO_2-reforming of methane over Pt/ZrO_2, Pt/CeO_2, $Pt/La–ZrO_2$ and $Pt/Ce_xZr_{1-x}O_2$ catalysts [13–15]. A rapid deactivation of the Pt/Al_2O_3 catalyst was observed whereas doped zirconia and ceria supported Pt catalysts were remarkably stable. A two-step mechanism was proposed to explain the promotional effect of the support on the CO_2-reforming of methane. The

first reaction path comprehends the decomposition of CH_4 on the metal particle, resulting in the formation of carbon and hydrogen. Carbon formed can partially reduce the support near the metal particles. The second path is the dissociation of CO_2 on the support followed by the formation of CO and O, which can reoxidize the support.

In this work, for the Pt/Al_2O_3 (973) and Pt/ZrO_2 catalysts, the increase of carbon deposits around or near the particle metal affects the CO_2 dissociation and inhibits methane conversion, and consequently the CO_2-reforming step of the partial oxidation of methane reaction. On the $Pt/Ce_{0.75}Zr_{0.25}O_2$ catalyst, the selectivity towards CO practically have not changed during reaction due to the redox mechanism of carbon removal promoted by the support.

3.3.2.5. Pulses of either CH_4 or O_2. Pulses of either CH_4 or O_2 were performed on the catalysts to investigate their capacity to remove the carbon of the catalyst surface. Figs. 10–13 show the consumption of CH_4, the H_2, the CO and the CO_2 production, respectively, over Pt/Al_2O_3 (973), Pt/ZrO_2 and $Pt/Ce_{0.75}Zr_{0.25}O_2$ catalysts.

During the first set of CH_4 pulses, only H_2 and CO were produced over all catalysts. The H_2 was formed from methane dissociation. Since there is no oxygen gas-phase species on the system, CO should be formed by the reaction between carbon from methane dissociation and oxygen from the supports ZrO_2 and $Ce_{0.75}Zr_{0.25}O_2$. Fathi et al. [32] observed, during CH_4 pulses on Pt/CeO_2 and $Pt/CeO_2/Al_2O_3$ catalysts at 973 K, that a fraction of H_2 produced was trapped on the support, forming hydroxyls on the surface. Then, in this work, the CO produced over Pt/Al_2O_3 could be attributed to the reaction between carbon from methane dissociation and the hydroxyls formed on the Al_2O_3 surface.

The consumption of CH_4, the H_2 and the CO production were higher for $Pt/Ce_{0.75}Zr_{0.25}O_2$ catalyst. This result suggests that the higher activity of $Pt/Ce_{0.75}Zr_{0.25}O_2$ catalyst is related to the capacity of this support to remove the carbon of the catalyst surface. During O_2 pulses, no H_2 was produced. CO and CO_2 were formed only during the first O_2 pulses over all catalysts. The amount of CO produced was higher over $Pt/Ce_{0.75}Zr_{0.25}O_2$ catalyst, while the Pt/Al_2O_3 (973) displayed the highest CO_2 production.
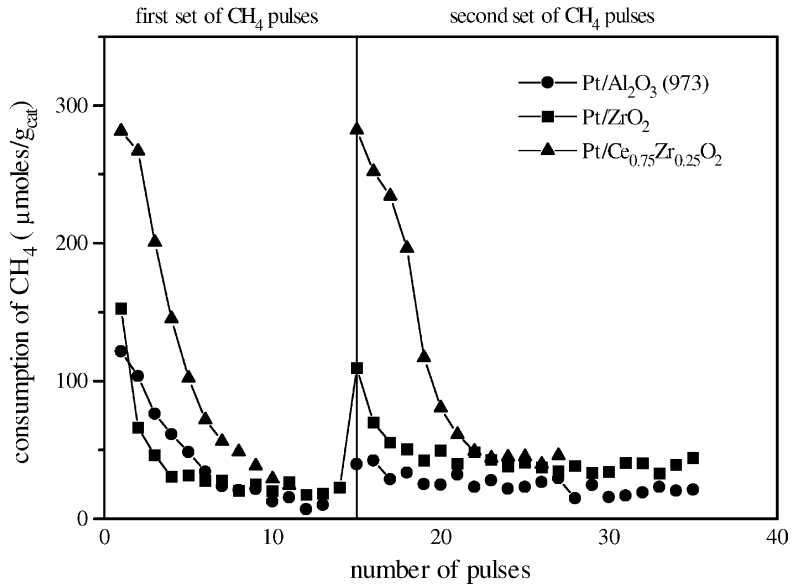
Fig. 10. Consumption of CH_4 during pulses of CH_4 at 1073 K over Pt/Al$_2$O$_3$ (973), Pt/ZrO$_2$ and Pt/Ce$_{0.75}$Zr$_{0.25}$O$_2$ catalysts.

The effects of the removal of carbon were observed in the second set of CH_4 pulses. During this set of CH_4 pulses, the Pt/Ce$_{0.75}$Zr$_{0.25}$O$_2$ catalyst had significantly higher activity than Pt/ZrO$_2$ and Pt/Al$_2$O$_3$ (973) catalysts. Furthermore, H_2 and CO were the only products

observed on Pt/ZrO$_2$ and Pt/Al$_2$O$_3$ (973) catalysts and these selectivities sharply decreased as the number of pulses increased. On the other hand, in the first few pulses, CO_2 and H_2O were also formed in addition to CO and H_2 on the Pt/Ce$_{0.75}$Zr$_{0.25}$O$_2$ catalyst.
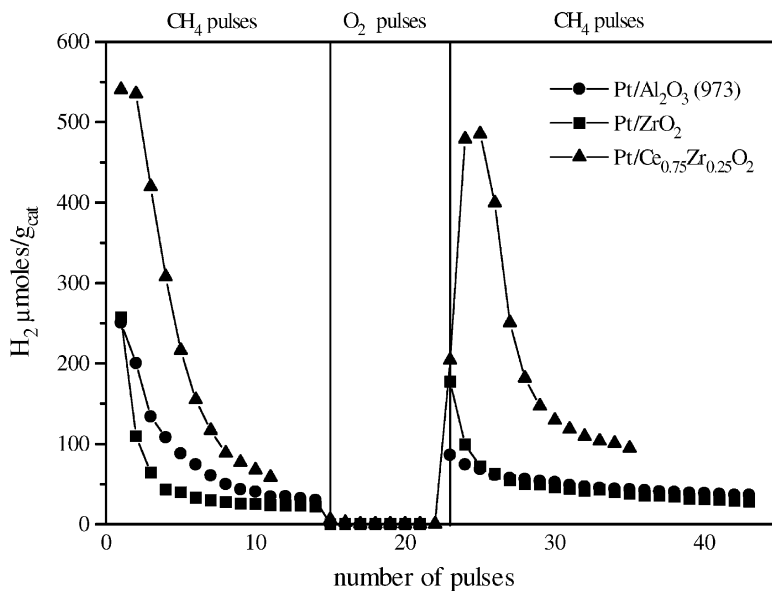

Fig. 11. H_2 production during pulses of either CH_4 or O_2 at 1073 K over Pt/Al$_2$O$_3$ (973), Pt/ZrO$_2$ and Pt/Ce$_{0.75}$Zr$_{0.25}$O$_2$ catalysts.
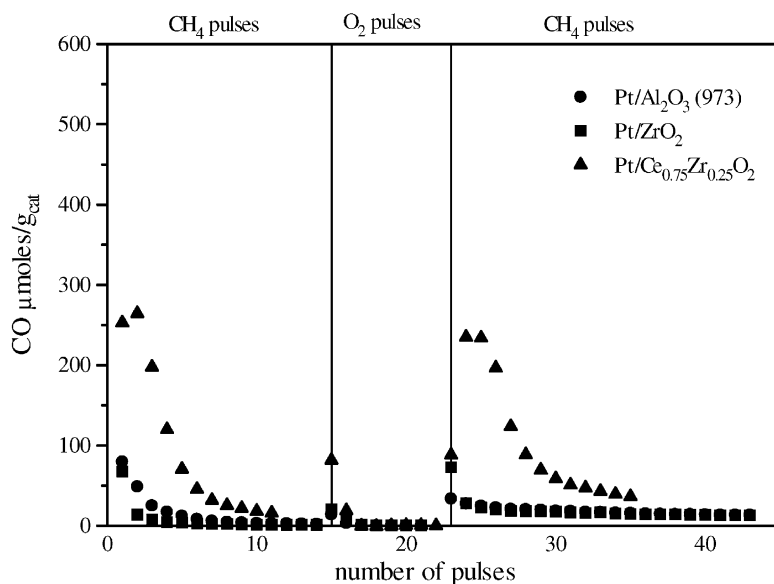
Fig. 12. CO production during pulses of either CH_4 or O_2 at 1073 K over Pt/Al_2O_3 (973), Pt/ZrO_2 and $Pt/Ce_{0.75}Zr_{0.25}O_2$ catalysts.

The selectivities to CO and H_2 achieved a maximum around the third pulse and then sharply decreased. Pantu et al. [33] also observed the same results when CH_4 pulses experiments were performed on Pt/CeO_2 and $Pt/Ce_{0.50}Zr_{0.50}O_2$ catalysts. The methane conversion decreased and CO selectivity increased as the number of CH_4 pulses increased. According to them, the reaction results on complete oxidation of methane until a certain degree of reduction has been reached after which the selectivity to CO rapidly increases. In our
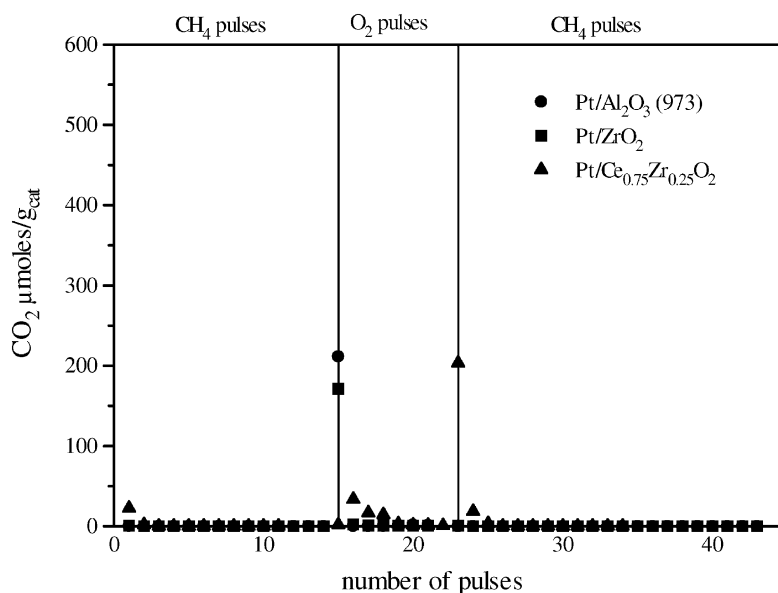

Fig. 13. CO_2 production during pulses of either CH_4 or O_2 at 1073 K over Pt/Al_2O_3 (973), Pt/ZrO_2 and $Pt/Ce_{0.75}Zr_{0.25}O_2$ catalysts.

work, the $Pt/Ce_{0.75}Zr_{0.25}O_2$ catalyst presents a much higher reduction degree than Pt/ZrO_2 and Pt/Al_2O_3 (973) catalysts as revealed by the OSC experiments.

The CH_4 consumption, the H_2 production and the CO formation decreased for all catalysts in comparison to the results obtained during the first set of CH_4 pulses. However, this effect was more pronounced on Pt/Al_2O_3 (973) catalyst, which presented a very low CH_4 consumption, H_2 production and CO formation.

These results agree with those reported by Stagg-Williams et al. [15] for Pt/ZrO_2 and $Pt/Ce–ZrO_2$ catalysts, during a sequence of $CH_4/CO_2/CH_4$ pulses. These experiments were done at the same conditions used in this work. They observed that, during the first set of CH_4 pulses, the Ce-doped catalyst produced the highest amount of H_2 and CO. During CO_2 pulses, oxygen support was replenished but the H_2 and CO production, on the second set of CH_4 pulses, were higher on $Pt/Ce–ZrO_2$ catalysts. They concluded that a higher degree of reduction results in an increase of the number of oxygen vacancies near the metal particle and a subsequent increase in the ability to clean the carbon formed on the metal particles. A similar mechanism was proposed by Pantu et al. [33]. According to these authors, the carbon formed from methane dissociation is either oxidized by lattice oxygen at or near the contact perimeter between the support and platinum particles or produce an inactive carbon. In this work, the results indicate that the oxygen vacancies of ZrO_2 and $Ce_{0.75}Zr_{0.25}O_2$ support were partially replenished during O_2 pulses, suggesting that the reduction degree of the support plays an important role on the reaction mechanism.

These findings are consistent with TPR and OSC results. As shown in Fig. 2 and Table 1, the $Pt/Ce_{0.75}Zr_{0.25}O_2$ catalyst exhibited a higher reducibility. Many studies [13,17–20] showed that the incorporation of Zr into the CeO_2 lattice increase the reducibility of this material. This enhancement of the reducibility can be attributed to an increase of oxygen mobility in the bulk of the mixed oxide.

4. Conclusions

Partial oxidation of methane proceeds through a two-step route on platinum supported catalysts. First, combustion of methane takes place, producing CO_2 and H_2O, then, synthesis gas is produced via carbon dioxide and steam-reforming reaction of unreacted methane. The reaction is favored for samples with higher dispersion. $Pt/Ce–ZrO_2$ was more active, stable and selective for partial methane oxidation than Pt/Al_2O_3 and Pt/ZrO_2 catalysts. This result may be explained by the higher reducibility and oxygen exchange capacity of $Pt/Ce–ZrO_2$ catalysts, which provided a mechanism for removing carbonaceous deposits from the active sites.

Acknowledgements

References

[1] V.K. Venkataraman, H.D. Guthrie, R.A. Avellanet, D.J. Driscoll, Stud. Surf. Sci. Catal. 119 (1998) 913.

[2] D. Dissanayake, M.P. Rosynek, K.C.C. Kharas, J.H. Lunsford, J. Catal. 132 (1991) 117.

[3] P.D.F. Vernon, M.L.H. Green, A.K. Cheetham, A.T. Ashcroft, Catal. Lett. 6 (1990) 181.

[4] D.A. Hickman, L.D. Schmidt, Science 259 (1993) 343.

[5] D.A. Hickman, E.A. Haupfear, L.D. Schmidt, Catal. Lett. 17 (1993) 223.

[6] D.A. Hickman, L.D. Schmidt, J. Catal. 138 (1992) 267.

[7] P.M. Torniainen, X. Chu, L.D. Schmidt, J. Catal. 146 (1994) 1.

[8] A.K. Bhattacharya, J.A. Breach, S. Chand, D.K. Ghorai, A. Hartridge, J. Keary, K.K. Mallick, Appl. Catal. A 80 (1992) L1.

[9] H. Dong, Z. Shao, G. Xiong, J. Tong, S. Sheng, W. Yang, Catal. Today 67 (2001) 3.

[10] M. Prettre, C. Eichner, M. Perrin, Trans. Faraday Soc. 43 (1946) 335.

[11] A.T. Ashcroft, A.K. Cheetham, J.S. Ford, M.L.H. Green, C.P. Grey, A.J. Murrell, P.D.F. Vernon, Nature 344 (1990) 319.

[12] F. van Looij, E.R. Stobbe, J.W. Geus, Catal. Lett. 50 (1998) 59.

[13] F.B. Noronha, G. Fendley, R.R. Soares, W.E. Alvarez, D.E. Resasco, Chem. Eng. J. 11 (2001) 3775.

[14] S.M. Stagg-Williams, D.E. Resasco, Stud. Surf. Sci. Catal. 119 (1998) 813.

[15] S.M. Stagg-Williams, F.B. Noronha, G. Fendley, D.E. Resasco, J. Catal. 194 (2000) 240.

[16] C.E. Hori, H. Permana, K.Y. Ng Simon, A. Brenner, K. More, K.M. Rahmoeller, D. Belton, Appl. Catal. B 16 (1998) 105.

[17] J. Kaspar, P. Fornasiero, M. Graziani, Catal. Today 50 (1999) 285.

[18] F. Fally, V. Perrichon, H. Vidal, J. Kaspar, G. Blanco, J.M. Pintado, S. Bernal, G. Colon, M. Daturi, J.C. Lavalley, Catal. Today 59 (2000) 373.

[19] H. Vidal, J. Kaspar, M. Pijolat, G. Colon, S. Bernal, A. Cordón, V. Perrichon, F. Fally, Appl. Catal. B 27 (2000) 49.

[20] H. Vidal, J. Kaspar, M. Pijolat, G. Colon, S. Bernal, A. Cordón, V. Perrichon, F. Fally, Appl. Catal. B 30 (2001) 75.

[21] M.H. Yao, R.J. Baird, F.W. Kunz, T.E. Hoost, J. Catal. 166 (1997) 67.

[22] E. Ruckenstein, H. Wang, J. Catal. 187 (1999) 151.

[23] S. James, http://www.fuelcelltoday.com/FuelCellToday/FCT FCTFiles/FCTArticleFiles/article_319_jamessunfuel processing0901.pdf, 2001.

[24] S.S. Bharodwaj, L.D. Schmidt, Fuel Process. Technol. 42 (1995) 109.

[25] M.C.J. Bradford, M.A. Vannice, Appl. Catal. 142 (1996) 97.

[26] J.H. Edwards, A.M. Maitra, Fuel Process. Technol. 42 (1995) 269.

[27] F. Solymosi, G. Kutsán, A. Erdohelyi, Catal. Lett. 11 (1991) 149.

[28] K. Seshan, H.W. ten Barge, W. Hally, A.N.J. van Keulen, J.R.H. Ross, Stud. Surf. Sci. Catal. 81 (1994) 285.

[29] J.R.H. Ross, A.N.J. van Keulen, M.E.S. Hegarty, K. Seshan, Catal. Today 30 (1996) 193.

[30] J.A. Lercher, J.H. Bitter, W. Hally, W. Niessen, K. Seshan, Stud. Surf. Sci. Catal. 101 (1996) 463.

[31] S.M. Stagg-Williams, E. Romeo, C. Padro, D.E. Resasco, J. Catal. 178 (1998) 139.

[32] M. Fathi, E. Bjorgum, T. Viig, O.A. Rokstad, Catal. Today 63 (2000) 489.

[33] P. Pantu, K. Kim, G.R. Gavalas, Appl. Catal. A 193 (2000) 203.